Fluctuations of the Au-Si(100) Schottky Barrier Height

H. Palm, M. Arbes, and M. Schulz
Institut für Angewandte Physik, Universität Erlangen-Nürnberg, D-91058 Erlangen, Germany
(Received 26 April 1993)

Schottky barrier height fluctuations of Au films on Si(100) are directly imaged with nm-scale resolution by ballistic electron emission. Fluctuations are made visible by using a highly doped ($N_d \approx 10^{17}$ cm^{-3}) substrate. Randomly distributed (approximately 10^{13} cm^{-2}) spots (about 2 nm in diameter) of reduced barrier height (typical $\Delta\Phi = 20$–50 meV) are observed. The microscopic distribution of barrier heights effective in emission is consistent with mean barrier height values measured by standard techniques.

PACS numbers: 61.16.–d, 68.35.–p, 73.30.+y, 73.40.Ns

Fluctuations in the Schottky barrier height (SBH) of metal-semiconductor contacts have recently been thoroughly discussed in the literature [1,2], because their existence plays a key role in the test of Schottky barrier (SB) models [3,4]. Up to now SBH fluctuations have not been directly imaged; however, many anomalies in experiments on SB contacts may be understood in terms of SBH inhomogeneities, e.g., an ideality factor greater than unity or discrepancies between SBH values determined by different measurement techniques [2].

In the present work, we show direct images of SBH fluctuations. We employ a combination of ballistic electron emission microscopy (BEEM) and ballistic electron emission spectroscopy (BEES) [5–7] in a pixel-by-pixel evaluation procedure. The method was described and successfully applied to an image in nanometer microscopy of the SBH of thin Au films on Si(111) in an earlier paper [8]. No significant fluctuations of the SBH were observed in these measurements. In the present work, we demonstrate the SBH fluctuations in excess of 0.3 eV are present in the SB at the Au-Si(100) interface; however, these fluctuations are only visible in highly doped samples causing high electric fields at the interface. In order to demonstrate this field effect in SBH imaging, we have applied nanometer microscopy of the SBH to two specific samples differing in the uniform substrate dopant concentration by almost 3 orders of magnitude. The two n-type (phosphorus) doping concentrations in Si(100) chosen are $N_d = 1.5\times10^{14}$ cm^{-3} and $N_d = 8.0\times10^{16}$ cm^{-3}. The procedure for the deposition of the thin Au film in order to prepare the Schottky contact was previously described in Ref. [8]. The Au contacts for the two samples are simultaneously fabricated to obtain comparable parameters, e.g., the Au film thickness $t_{Au} = 7.9$ nm and the typical Au grain diameter $d_{Au} \approx 20$ nm.

A commercial scanning tunneling microscope (STM) (Besocke walker type [9]) is used to perform BEEM and BEES measurements at room temperature. The tunneling injection current from a Pt-Ir tip is maintained constant at $I_t = 3$ nA. The collector current I_c analyzed in the range $0 \le I_c \le 100$ pA is converted to a voltage by a low-noise electrometer amplifier. The collector current is measured without an external substrate bias voltage. With a typical SBH for Au on n-Si(100) $\Phi_{Au} = 0.8$ eV, the interface electric field of the samples is estimated to be $F = 3.6\times10^3$ V/cm and $F = 1.1\times10^5$ V/cm for the low and high doping concentrations, respectively. In the following, we refer to the sample having the lower electric field as "LFLD" and to the other sample as "HFLD."

Images and histograms are determined by a combination of the BEEM and BEES methods in a pixel-by-pixel evaluation as described in Ref. [8]. Typically twelve BEEM images are taken at different tunneling bias voltages V_t in the range $0.5\ \text{V} \le V_t \le 1.2$ V to define BEES I_c-V_t characteristics for each pixel. The SBH Φ_{eff} effective in BEES is determined as the voltage offset for the collector current onset by applying a linear regression to the individual I_c-V_t characteristics. Using a square power law also proposed in the literature [10] for a narrow voltage region around the threshold of the collector current yields similar image information. The magnitude of the effective SBH determined by the linear and the quadratic power law varies by less than 20 meV. For more than 95% of the pixels, we obtain a good regression coefficient r in the range $0.95 \le r \le 1$. A pixel is defined to be a dead element when the regression coefficient determined is outside this range. These dead elements usually correlate with a low collector current $I_c \le 2$ pA.

Figures 1(a) and 1(b) show typical images of the effective SBH Φ_{eff} for the two samples. The image areas are 60×60 nm in both cases. The contrast ranges from 0.6 eV (black) $\le \Phi_{eff} \le$ 1.0 eV (white). Dead elements are depicted in white so that they are clearly visible in the images. The LFLD sample in Fig. 1(a) in general shows less contrast variation than the HFLD sample in Fig. 1(b). Figure 1(b) exhibits a large number (density approximately 10^{13} cm^{-2}) of dark spots. The average spot diameter is $d \approx 2$ nm. The peak barrier height reduction in the spots ranges up to more than 100 meV. Typical reduction values range within 20–50 meV. In the lower right corner, there appears to be an extended area of a reduced barrier height. Neither the dark spots nor the extended area of reduced barrier height can be correlated with the island structure of the Au film characterized by

0031-9007/93/71(14)/2224(4)$06.00

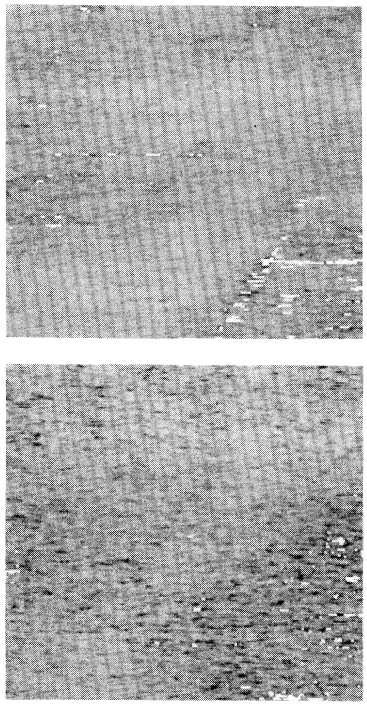

FIG. 1. Images of the effective Schottky barrier height Φ_{eff}. The image area is 60×60 nm covered by 512×512 pixels. The image contrast window is 0.6 eV (black) $\leq \Phi_{\text{eff}} \leq$ 1.0 eV (white). Dead pixels are depicted white. (a) Low-field sample LFLD. (b) High-field sample HFLD.

a standard STM image.

It is noted that the image spots extend over approximately 15×15 pixels and are not caused by noise in the image. The slight stretch out of the spots in the horizontal scan direction is an artifact of the measurement response time. The spot pattern appears to be caused by randomly distributed defects in the interface region causing a SBH reduction. The density of these defects is more than 2 orders of magnitude larger than the area density (approximately 10^{11} cm^{-2}) of doping centers in the interface region of 10 nm depth.

Quantitative information on the effective barrier height can be extracted from the histograms shown in Fig. 2. The histograms of Fig. 2 show the same data as in Fig. 1; only dead elements are excluded. The barrier height distributions are smooth with only one maximum, thus indicating a well defined mean barrier height smeared out by statistical fluctuations. The maxima yield the most probable barrier height magnitudes $\Phi_{\text{LFLD,max}}$ =825 meV and $\Phi_{\text{HFLD,max}}$ =801 meV for the LFLD and HFLD cases, respectively. The shift $\Delta = 24 \pm 10$ meV of the maximum to a lower barrier height value at high fields is within the error in accordance with the lowering Δ_{SE} =31 meV due to the Schottky effect. A noticeable fraction (5–10 meV) of the mean barrier lowering is estimated to be caused by

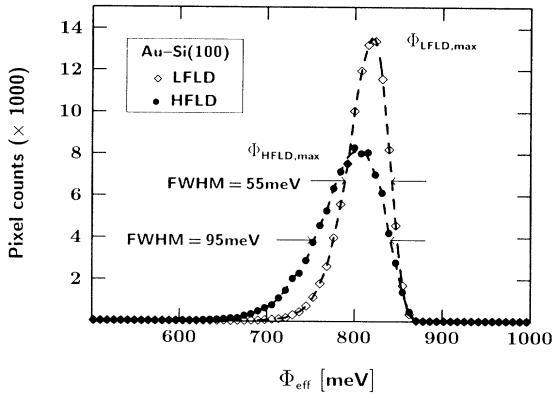

FIG. 2. Histograms of the effective barrier height Φ_{eff} for the two samples LFLD and HFLD. Dead elements are not included. The main parameters of the distribution are indicated by the curves.

the barrier reduction in the spots.

It is also noted that the width of the distribution is increased for the HFLD case. The value of the full width at half maximum is almost doubled from FWHM (LFLD) =55 meV $\approx 2k_BT$ to FWHM(HFLD) =95 meV. The HFLD distribution also shows a long tail towards low barriers in an asymmetric distribution. The width of the distribution in the LFLD case is of the order of thermal broadening which limits the barrier height measurements [10]. Figure 1(a) of the LFLD sample also shows a similar spotlike structure as Fig. 1(b) of the HFLD sample; however, the magnitude of this structure cannot be clearly distinguished from thermal noise. The increased broadening in the HFLD case is significantly larger than the thermal broadening. We interpret this broadening by barrier height fluctuations which are present in the Au-Si(100) interface. Since both samples are fabricated in the same way, the fluctuations are most probably present in both samples but only clearly visible in the HFLD sample.

The magnitude of the effective barrier height fluctuations observed in BEEM measurements is discussed on the basis of the inhomogeneous band bending as reported in the literature [1,2] together with an additional effective barrier lowering due to the Schottky effect [11]. The barrier lowering effects are depicted in Fig. 3. The magnitude of the effective barrier height and the lowering for the LFLD and HFLD samples are calculated for a uniform metal-semiconductor interface barrier height Φ_{B0} =800 meV superimposed by a constant lowering Δ_{IF} =300 meV assumed in the shape of a circular patch of d =2 nm diameter in accordance with the spot diameter observed in the image Fig. 1(b). The dotted lines indicate the triangular band bending outside the patch for the two doping concentrations of our samples (LFLD,HFLD) extrapolated to the interface. The dash-dotted curves show the band bending along a line normal to the inter-

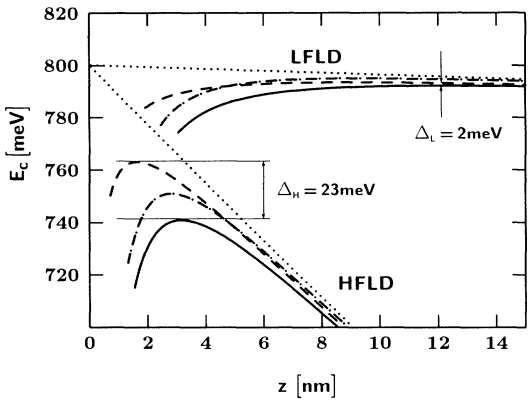

FIG. 3. Calculated band bending E_c as a function of depth z normal to the interface for the LFLD and the HFLD sample. The dotted curves indicate the ideal triangular profiles. The dash-dotted curves show the band bending normal to a circular patch of 2 nm in diameter having a reduced interface barrier height of 500 meV. The dashed lines and the continuous lines are determined by superposition of the image force potential with the dotted and the dash-dotted curves, respectively. The effective barrier height differences Δ_L and Δ_H due to the interface barrier height variation are indicated for the LFLD and the HFLD case.

face from the center of the circular patch into the semiconductor space charge region. The dash-dotted curves are calculated by solving Poisson's equation [Eq. (6) in Ref. [1]]. An effective barrier height occurs at the band bending maximum inside the space charge region. An additional band bending is due to the Schottky effect induced by the image force potential [11]. The total band bending outside the patch is shown in Fig. 3 by the dashed lines and at the center position of the patch by the continuous lines. The effective barrier is located approximately 12 nm below the interface in the space charge region for the LFLD sample. At this distance the interface barrier lowering $\Delta_{IF} = 300$ meV has almost completely decayed. The barrier height variation $\Delta_L \approx 2$ meV between the band bending maxima inside and outside the patch is marginal. Therefore, it is not possible to detect interface barrier fluctuations using low-doped semiconductor substrates.

In the HFLD case, the effective barrier maximum is moved close (≈ 2 nm) to the interface. The residual barrier height variation is $\Delta_H = 23$ meV. The lowering due to the Schottky effect compared to the LFLD case is 31 meV. This Schottky effect barrier lowering is directly visible in the experimentally observed shift of the HFLD distribution maxima of 24 ± 10 meV. The calculated value is in accordance with the experimental value. The measurement of the Schottky effect by ballistic electron emission with the BEEM technique is in agreement with the classical photoelectric measurements on Schottky barriers [12].

The effective barrier height variation Δ_H in Fig. 3 is chosen to be within the magnitude range of typical barrier lowering values observed in the spots of Fig. 1(b). A rather small value was picked from the range in order to estimate a lower limit of the interface barrier height deviation. In general, the knowledge of the effective barrier height variation Δ_H and Δ_L is not sufficient to extrapolate back to an abrupt metal-semiconductor interface barrier height variation Δ_{IF}, because the decay of interface fluctuations to the position of the effective barrier depends on the individual characteristics of the fluctuation, e.g., on the diameter of the circular patch. In our measurement, however, we are able to determine the characteristic fluctuation length from the spot diameter $d \approx 2$ nm in the image Fig. 1(b). This diameter is applied in the calculation of the band bending in Fig. 3; therefore, the extrapolated interface variation $\Delta_{IF} = 300$ meV is a low estimate of the deviation in the interface barrier. The spots having an effective barrier lowering in excess of 100 meV lead to interface barrier lowerings larger than the SBH. For such a large fluctuation the extrapolation to a planar interface is not valid. This discrepancy, the magnitude of the barrier lowering, and the spotlike appearance of the observed fluctuations may well be explained by defects distributed a few nanometers from the interface into the semiconductor; however, we cannot rule out an interface roughness as the origin of the fluctuations. For a discussion of the origin of these fluctuations and the consequences on SB models further information on the interface structure is necessary.

TABLE I. Barrier height values $\Phi_{I\text{-}V}$, Φ_{PE}, and $\Phi_{C\text{-}V}$ as determined from I-V, photoelectric, and C-V measurements, respectively, and weighted averages for the two samples LFLD and HFLD.

Sample	Method	$\Phi_{I\text{-}V}$ (meV)	Φ_{PE} (meV)	$\Phi_{C\text{-}V}$ (meV)
LFLD	Experimental	803 ± 20	816 ± 15	837 ± 25
	Weighted average	799	820	835
HFLD	Experimental	722 ± 20	770 ± 15	835 ± 25
	Weighted average	711	780	843

The histograms in Fig. 2 may be regarded as probability distributions of the effective barrier height. These probability distributions can be used to calculate weighted averages of the effective barrier height as they are observed in various measurement methods. In the following, we perform these evaluations to compare our BEEM barrier height data with the mean barrier height values obtained by the standard capacitance-voltage (C-V), the current-voltage (I-V), and the photoelectric (PE) measurements performed on the same HFLD and LFLD samples as used in the BEEM measurements. The barrier height values experimentally determined by the different methods are listed in Table I for the LFLD and the HFLD samples, respectively. The experimental methods chosen for the comparison characteristically

differ in the weighting of the average formation. The current in thermionic emission across a barrier Φ_{eff} is exponentially weighted by the Boltzmann factor $w_{I\text{-}V} = \exp[-\Phi_{\text{eff}}/k_B T]$ [13]. The barrier height determination by photoelectric measurement takes an average value with a weighting $w_{\text{PE}} = (h\nu - \Phi_{\text{eff}})^2$ according to the Fowler model of internal photoemission [14] where $h\nu$ is the photon energy in the measurement range. In the C-V measurement, the mean barrier height is determined; however, an image force is not present. The average BEEM barrier height value must therefore be corrected by the Schottky effect lowering.

The barrier height values calculated from the histograms with the appropriate weighting factors are listed in Table I together with the experimentally determined barrier heights for the LFLD and HFLD samples. The experimentally determined barrier height values differ considerably for the various measurement techniques; the $\Phi_{C\text{-}V}$ and $\Phi_{I\text{-}V}$ barrier height magnitudes for the HFLD sample differ by more than 100 meV. The barrier height values calculated from the histograms reflect the trends of the barrier lowering very well and quantitatively agree with the measured values within the measurement error (standard deviation). The comparison shows that the different weighting by which barrier height fluctuations affect the various measurement methods leads to a large scatter of the mean barrier height values. The effect is especially strong for the I-V measurement for which regions of low barrier height are favored by the exponential weighting. The barrier height fluctuations strongly affect the barrier height determination when high fields are present at the interface either induced by a high doping concentration or by a reverse bias voltage applied. In the measurements, we have therefore limited the bias variation to a narrow range to make the comparison valid. Only slightly differing mean barrier height values are determined in the LFLD case.

In summary, we have shown a direct image of Schottky barrier height fluctuations by a pixel-by-pixel evaluation of ballistic electron emission microscopy measurements. The fluctuations are made visible by using a highly doped semiconductor substrate. The high doping concentration shifts the barrier effective in emission very close (approximately 2 nm) to the interface. The effect is demonstrated by comparing the results of a high- and a low-doped sample. The barrier height image shows nanometer-size spots with a reduced barrier which are not correlated with the island structure of the metal film. The magnitude of the fluctuations and their spotlike appearance indicate a distribution of defects from the interface a few nanometers into the semiconductor. The microscopic barrier height distribution measured by BEEM is used to calculate weighted averages of barrier heights as determined in standard macroscopic measurements. Quantitative agreement is obtained with measured data.

This work was supported by the Deutsche Forschungsgemeinschaft through SFB292.

[1] R. T. Tung, Phys. Rev. B **45**, 13509 (1992).
[2] J. P. Sullivan, R. T. Tung, M. R. Pinto, and W. R. Graham, J. Appl. Phys. **70**, 7403 (1991).
[3] W. E. Spicer, I. Lindau, P. Skeath, and C. Y. Su, J. Vac. Sci. Technol. **17**, 1019 (1980).
[4] G. P. Das, P. Blöchl, O. K. Andersen, N. E. Christensen, and O. Gunnarsson, Phys. Rev. Lett. **63**, 1168 (1989).
[5] W. J. Kaiser and L. D. Bell, Phys. Rev. Lett. **60**, 1406 (1988).
[6] M. H. Hecht, L. D. Bell, W. J. Kaiser, and F. J. Grunthaner, Appl. Phys. Lett. **55**, 780 (1989).
[7] M. Prietsch and R. Ludeke, Phys. Rev. Lett. **66**, 2511 (1991).
[8] H. Palm, M. Arbes, and M. Schulz, Appl. Phys. A **56**, 1 (1993).
[9] K. Besocke, Surf. Sci. **181**, 145 (1987).
[10] L. D. Bell, W. J. Kaiser, M. H. Hecht, and L. C. Davis, J. Vac. Sci. Technol. B **9**, 594 (1991).
[11] V. L. Rideout, Thin Solid Films **48**, 261 (1978).
[12] S. M. Sze, C. R. Crowell, and D. Kahng, J. Appl. Phys. **35**, 2534 (1964).
[13] E. H. Rhoderick and R. H. Williams, *Metal-Semiconductor Contacts* (Clarendon, Oxford, 1988).
[14] R. H. Fowler, Phys. Rev. **38**, 45 (1931).

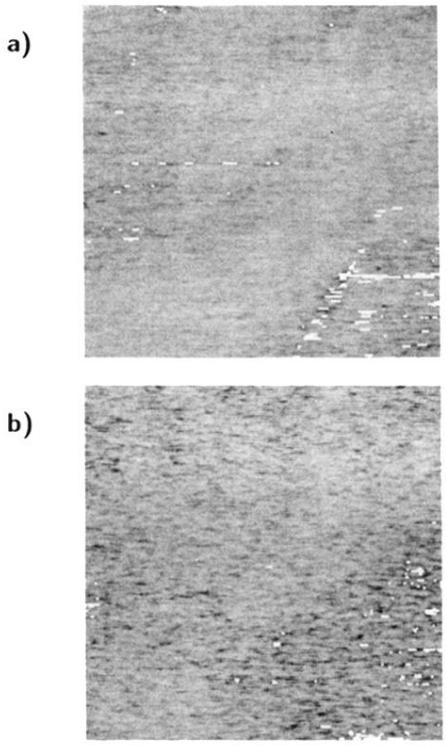

FIG. 1. Images of the effective Schottky barrier height Φ_{eff}. The image area is 60×60 nm covered by 512×512 pixels. The image contrast window is 0.6 eV (black) $\leq \Phi_{eff} \leq$ 1.0 eV (white). Dead pixels are depicted white. (a) Low-field sample LFLD. (b) High-field sample HFLD.